Frequency Analysis of Fluid-Structure systems using NEM

F. Daneshmand
Mechanical Engineering Department, School of Engineering, Shiraz 71345, Iran
Corresponding author. Tel. : +987112303051; fax: +987116287508.
daneshmd@shirazu.ac.ir

A. Shekari
Mechanical Engineering Department, School of Engineering, Shiraz 71345, Iran
Corresponding author. Tel. : +987112303051; fax: +987116287508.
ar_shekari@yahoo.com

Abstract. NEM is a meshless numerical method for the solution of partial differential equations. In this paper the application of the NEM to boundary value problems in two dimensional small displacement fluid-structure interaction is presented. In the natural element method, the approximate functions are constructed using natural neighbor interpolants. These interpolants are based on the Voronoi tessellation of the set of nodes N. In one-dimensional, NEM is identical to linear finite elements. The NEM interpolant is strictly linear between adjacent nodes on the boundary of the convex hall, which fascilates imposition of the essential boundary conditions. A standard Galerkin procedure is used to obtain the discrete system of linear equations. Application of the NEM to a dam-reservoir system and two types of tanks is presented. The obtained results using NEM are compared with others solution. Excellent agreement with previous solution is obtained, which exemplifies the accuracy and robustness of NEM and suggests its potential application in other classes of problems e.g. the problems with large deformations. Two examples are solved: the free vibrations of a Pine Flat dam-reservoir system and two types of tanks. The computed results using NEM are compared with the results obtained by finite element method.

Keywords. NEM, meshless, fluid-structure interaction, dam-reservoir, displacement potential.

Introduction

The hydrodynamic response analysis of many practical engineering problems, such as a dam-reservoir system differs from that of any other ground structure. It is because the hydrodynamic pressures modify the dam deformations, which in turn modify the hydrodynamic pressure causing them. It means that the fluid–structure interaction can significantly affect the dynamic response of the dams and needs to be properly taken into account in the analysis.

One of the first meshless methods proposed is the Smooth Particle Hydrodynamics (SPH) (Monaghan 1988), which was the basis for a more general method known as the Reproducing Kernel Particle method (RKPM) (Liu et al. 1995). Starting from a completely different and original idea, the Moving Least Squares shape function (MLSQ) (Nayroles et al. 1992) has become very popular in the meshless community. More recently, the equivalence between MLSQ and RKPM has been proven, so that both methods may now be considered to be based on the same shape functions (Aluru and Li 2001). The MLSQ shape function has been successfully used in a weak form (Galerkin) with a background grid for the integration domain (Nayroles et al. 1992, Belytschko et al. 1994 a,b). Onate et al. (1996 a,b) used MLSQ in a strong form (Point Collocation) avoiding the background grid. Liu et al. (1995 a,b) have used the RKPM in a weak form, while Aluru [2000] used it in a strong form. Other authors use different integration rules or weighting functions [De and Bathe 2000, Atluri and Zhu 2000] with the same shape functions.

A newcomer meshless method is the Natural Element Method (NEM). This method is based on the natural neighbor concept to define the shape functions (Sibson 1980). NEM has been used with a weak form (Sukumar et al. 2001). The main advantage of this method over the previously used meshless methods is the use of Voronoi diagrams to define the shape functions, which yields a very stable partition. The added advantage is the capability for nodal data interpolation, which facilitates a mean to impose the essential boundary conditions. Finally, all the shape functions, including the FEM shape functions, may be defined as Partition of Unity approximations (Babuska and Melenk 1995, Cueto et al. 2003, Alfaro et al. 2005). Several other shape functions may also be developed using this concept.

Natural neighbour-based interpolants

Voronoi diagram and Delaunay triangulation

Consider a bounded domain Ω in *d*-dimensions described by a set **N** of *M* scattered nodes: **N** = {n_1, n_2, . . . , n_M}. The Voronoi diagram $\upsilon(\mathbf{N})$ of the set **N** is a subdivision of the domain into regions $V(n_I)$, such that any point in $V(n_I)$ is closer to node n_I than to any other node $n_J \in N(J \neq I)$. The region $V(n_I)$ (first-order Voronoi cell) for a node n_I within the convex hull is a convex polygon (polyhedron)

$$V(n_I) = \left\{ \mathbf{x} \in \mathbb{R}^d : d(\mathbf{x}, \mathbf{x}_I) < d(\mathbf{x}, \mathbf{x}_J) \; \forall J \neq I \right\} \tag{1}$$

Where $d(\mathbf{x}_I, \mathbf{x}_J)$ is an appropriate distance function (usually the standard Euclidean distance is used) between $\mathbf{x}_I$ and $\mathbf{x}_J$.

The dual of the Voronoi diagram, the Delaunay tessellation, is constructed by connecting nodes that have a common (*d*-1)-dimensional Voronoi facet. Given any nodal set **N**, the Voronoi diagram is unique, whereas the Delaunay tessellation is not (a simple example is the triangulation of a square where choosing either diagonal leads to two valid Delaunay triangulations). In Fig. 1a, the Voronoi diagram and the Delaunay triangulation are shown for a nodal set consisting of seven nodes (*M*=7). A Voronoi vertex and an edge are also indicated in this Fig 1a. An important property of Delaunay triangles is the empty circumcircle criterion. It means that if DT (n_J, n_K, n_L) is any Delaunay triangle of the nodal set **N**, then the circumcircle of *DT* contains no other nodes of **N.** In Fig 1b, the Delaunay circumcircles for three triangles are shown.

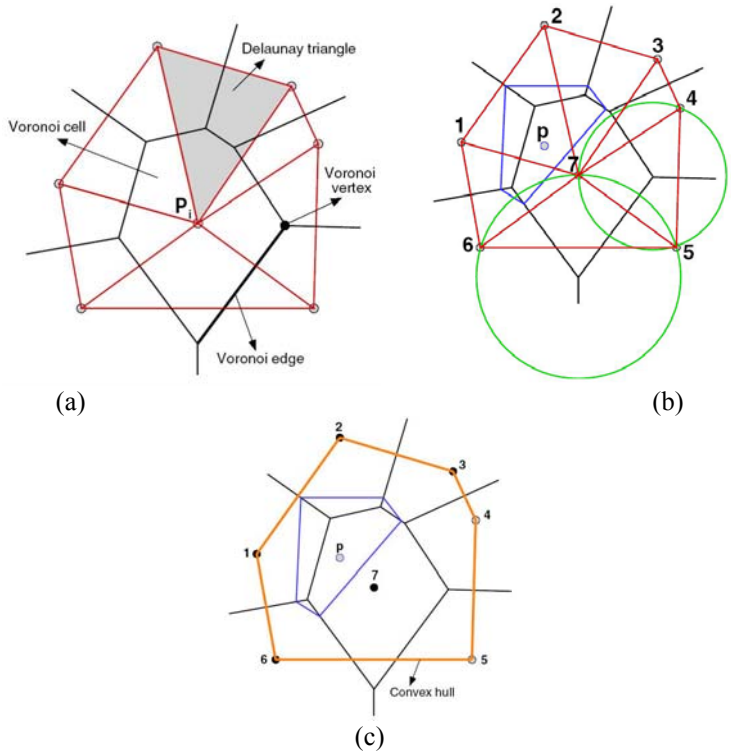

Figure 1. (a) Voronoi diagram and Delaunay triangulation; (b) Delaunay circumcircles; and (c) Natural neighbours (filled circles) of inserted point P.

Consider now the introduction of a point *p* with coordinates $\mathbf{x} \in \mathbb{R}^2$ into the domain Ω (Fig 1b). The Voronoi diagram $V(n_1, n_2, \ldots, n_M, p)$ or equivalently the Delaunay triangulation $DT(n_1, n_2, \ldots, n_M, p)$ for the *M* nodes and the point *p* is constructed. Now, if the Voronoi cell for *p* and n_I have a common facet (segment in $\mathbb{R}^2$ and polygon in $\mathbb{R}^3$), then the node n_I is said to be a *natural neighbor* of the point *p*. The Voronoi cells for the point *p* and its natural neighbors are shown in Fig 1c, together with the convex hull of the set of points.

Sibson interpolation

The natural neighbor (Sibson) interpolant was introduced by Sibson. For simplicity and ease of exposition, we restrict our attention to 2-dimensions, although every concept is easily extended to $d > 2$. The definition of the Voronoi diagram (first-order) appears in equation (1). By a similar extension, one can construct higher order (*k*-order, $k > 1$) Voronoi diagrams in the plane. Of particular interest in the present context is the case $k = 2$, which is the second-order Voronoi diagram. The second order Voronoi diagram of the set of nodes **N** is a sub-division of the plane into cells V_{IJ},

such that V_{IJ} is the locus of all points that have n_I as the nearest neighbor, and n_J as the second nearest neighbor. The second-order Voronoi cell V_{IJ} (I ≠ J) is defined as

$$V_{IJ} = \left\{ \mathbf{x} \in \mathbb{R}^d : d(\mathbf{x}, \mathbf{x}_I) < d(\mathbf{x}, \mathbf{x}_J) < d(\mathbf{x}, \mathbf{x}_K) \; \forall K \neq I, J \right\} \qquad (2)$$

In order to quantify the neighbors for a point p with coordinate $\mathbf{x} = (x_1, x_2)$ that is inserted into the tessellation, Sibson used the concept of second-order Voronoi cells, and thereby introduced natural neighbors and natural neighbor coordinates. Natural neighbor coordinates (shape functions) are used as the interpolating functions in natural neighbor (Sibson) interpolation, and as trial and test functions in a Galerkin implementation for the solution of partial differential equations. Consider Fig 2a, where a point p is inserting into a tessellation. The natural neighbor shape function of p with respect to a natural neighbor I is defined as the ratio of the area of the second-order Voronoi cell (A_I) to the total area of the first-order Voronoi cell of p (A):

$$\phi_I(\mathbf{x}) = \frac{A_I(\mathbf{x})}{A(\mathbf{x})} \qquad A(\mathbf{x}) = \sum_{J=1}^{n} A_J(\mathbf{x}) \qquad (3)$$

where $n = 5$ for the point p in Fig 2a. In 3-d, the Sibson shape function is defined as the ratio of polyhedral volumes.

The derivatives of the Sibson shape functions are obtained by differentiating equation (3)

$$\phi_{I,j}(\mathrm{x}) = \frac{A_{I,j}(\mathrm{x}) - \phi_I(\mathrm{x}) A_{,j}(\mathrm{x})}{A(\mathrm{x})} \quad (j = 1,2) \qquad (4)$$

If the point $\mathbf{x} \to \mathbf{x}_I$, then $\phi_I(\mathbf{x}) = 1$ and all other shape functions are zero. Therefore, the properties of positivity, interpolation, and partition of unity are straightforward:

$$0 \le \phi_I \le 1, \quad \phi_I(\mathbf{x}_J) = \delta_{IJ}, \quad \sum_{I=1}^{n} \phi_I(\mathbf{x}) = 1 \qquad (5)$$

Natural neighbor shape functions also satisfy the local coordinate property, namely

$$\mathbf{x} = \sum_{I=1}^{n} \phi_I(\mathbf{x}) \mathbf{x}_I \qquad (6)$$

and hence in conjunction with the partition of unity property, it is readily derived that the Sibson interpolant can exactly represent any linear field which is known as linear completeness in the finite element method.

Governing equations for solid and fluid domains

Let Ω_s and Ω_f be the domains occupied by the solid and fluid respectively. The fluid and solid boundaries may be divided into four different parts according to their properties, the fluid-structure interface, Γ_1 with $\mathbf{n}$ its unit normal vector pointing outwards Ω_f, a free surface with prescribed external pressure, Γ_2, a surface with prescribed displacements as essential boundary conditions, Γ_3 and a traction free surface, Γ_4 with η its unit outward normal vector.

In the absence of external forces the governing equations for free motions of the system are as following:

The equation of motion for the solid domain is as follows

$$\nabla \cdot \boldsymbol{\sigma} + \rho_s \mathbf{b} = \rho_s \ddot{\mathbf{u}} \qquad (12)$$

Where $\mathbf{u}$ is the solid displacement, ρ_s is the density of solid, $\mathbf{b}$ is the body force vector and $\boldsymbol{\sigma}$ is the Cauchy stress tensor.

The equilibrium and state equations for an inviscid compressible fluid are written as

$$\rho_0 \frac{\partial \mathbf{v}}{\partial t} + \nabla p = 0 \qquad (13)$$

$$\frac{\partial p}{\partial t} + \rho_0 c^2 (\nabla . \mathbf{v}) = 0 \qquad (14)$$

Where $\mathbf{v}$ is the fluid velocity vector, ρ_0 is the reference density, p is the pressure in the fluid, and c is the speed of sound in the media. Assuming the irrotational flow, considering small amplitude motions and introducing displacement potential ψ and displacement field of the fluid $\mathbf{u_f}$ as

$$\mathbf{u_f} = \nabla \psi \qquad (15)$$

the following equation can be obtained

$$\frac{\partial^2 \psi}{\partial t^2} = c^2 \nabla^2 \psi \tag{16}$$

The boundary conditions for the solid domain are

$$\mathbf{u} = \mathbf{0} \qquad on\ \Gamma_3 \tag{17}$$

$$\bar{\mathbf{t}} = \boldsymbol{\sigma}\,\boldsymbol{\eta} = \mathbf{0} \quad on\ \Gamma_4 \tag{18}$$

Where $\bar{\mathbf{t}}$ is the prescribed traction on Γ_4. The required boundary condition on Γ_2 can be obtained using the linearized wave assumption as (Daneshmand and Niroomandi 2007)

$$g \nabla \psi \cdot \mathbf{n} = -\frac{\partial^2 \psi}{\partial t^2} - \frac{p_e}{\rho_0} \tag{19}$$

Natural element discretization

The derived equations in previous section are discretized in this section using natural element method. Using the Sibson shape functions, the displacement vector $\mathbf{u}^h(\mathbf{x},t)$ and the displacement potential $\psi^h(\mathbf{x},t)$ can be written as

$$\mathbf{u}^h(\mathbf{x},t) = \sum_{I=1}^{n} \phi_I(\mathbf{x})\, u_I(t) \tag{20}$$

$$\psi^h(\mathbf{x},t) = \sum_{I=1}^{n} \phi_I(\mathbf{x})\, \psi_I(t) \tag{21}$$

Where $\mathbf{u}_I\,(I = 1, 2, ..., n)$ and $\psi_I\,(I = 1, 2, ..., n)$ are the vector of nodal displacements and the displacement potentials at the n natural neighbours of point $\mathbf{x}$, respectively and $\phi_I(\mathbf{x})$ is the shape functions associated with each node. Note that the shape functions are time independent and the nodal displacements are functions of time only.

Solid Domain

The matrix equation for the solid is given by

$$\mathbf{M}_s \ddot{\mathbf{U}}_s + \mathbf{K}_s \mathbf{U}_s = \mathbf{L} \tag{22}$$

Where $\mathbf{U}$ is the vector including the unknown nodal values of the displacement, and $\mathbf{M}_s$ and $\mathbf{K}_s$ are the structural mass and stiffness matrix, respectively. $\mathbf{L}$ is the load vector includes both the external structural loads and the load vector due to coupling effects.

The $\mathbf{L}$ can be rewritten as

$$\mathbf{L} = \left(\int_{\Omega} \Phi_I \mathbf{b}\, d\Omega + \int_{\Gamma_t} \Phi_I \bar{\mathbf{t}}\, d\Gamma \right) - \left(\rho_0 \int_{\Gamma_1} \phi_I \mathbf{n}^T \phi_J d\Gamma \right) \ddot{\boldsymbol{\Psi}} = \mathbf{L}_s - \mathbf{M}_c \ddot{\boldsymbol{\Psi}} \tag{23}$$

The total assembled system of equations using the

$$\left(\mathbf{M}_s\right)_{IJ} = \int_{\Omega} \rho_s\, \phi_I \phi_J\, d\Omega \tag{24}$$

$$\left(\mathbf{K}_s\right)_{IJ} = \int_{\Omega} \mathbf{B}_I^T \mathbf{C}\, \mathbf{B}_J\, d\Omega \tag{25}$$

Where consistent mass matrix is used in calculating mass matrix, $\mathbf{C}$ is the constitutive matrix, and $\mathbf{B}_I$ is the matrix of shape function derivatives.

Fluid Domain

Using the test function $w = w(x, y)$, equation (16) can be integrated over the fluid domain to yield

$$\int_{\Omega} w\, \psi_{,tt}\, d\Omega = \int_{\Omega} w c^2 \nabla^2 \psi\, d\Omega \tag{26}$$

Using Green's formula on the right-hand side and rearranging

$$\rho_0 g\int_\Omega w\psi_{,tt}\,d\Omega+\rho_0 gc^2\int_\Omega(\nabla w)\cdot(\nabla\psi)\,d\Omega=\rho_0 gc^2\int_\Gamma w(\nabla\psi)\cdot\mathbf{n}\,d\Gamma$$
$$=c^2\left(\rho_0 g\int_{\Gamma_1} w u_{sf}\,d\Gamma-\rho_0\int_{\Gamma_2} w\psi_{,tt}\,d\Gamma-\int_{\Gamma_2} w\,p_e\,d\Gamma\right) \quad (27)$$

and finally,

$$\rho_0 g\int_\Omega w\psi_{,tt}\,d\Omega+\rho_0 gc^2\int_\Omega(\nabla w)\cdot(\nabla\psi)\,d\Omega$$
$$=\rho_0 gc^2\int_{\Gamma_1} w u_{sf}\,d\Gamma-c^2\int_{\Gamma_2} w(\rho_0\psi_{,tt}+p_e)d\Gamma \quad (28)$$

Choosing w according to the Galerkin method, the matrix form of equation (39) becomes

$$\mathbf{M}_f\ddot{\mathbf{\Psi}}+\mathbf{K}_f\mathbf{\Psi}=\mathbf{L}' \quad (29)$$

In which $\mathbf{\Psi}$ is the vector including the unknown nodal values of the displacement potential and

$$\left(\mathbf{M}_f\right)_{IJ}=\rho_0 g\int_\Omega\phi_I\phi_J\,d\Omega+\rho_0 gc^2\int_{\Gamma_2}\phi_I\phi_J\,d\Gamma \quad (30)$$

$$\left(\mathbf{K}_f\right)_{IJ}=\rho_0 gc^2\int_\Omega(\nabla\phi_I)^T(\nabla\phi_J)d\Omega \quad (31)$$

$$\mathbf{L}'=\rho_0 gc^2\int_{\Gamma_1}\phi_I\,u_{sf}d\Gamma-c^2\int_{\Gamma_2}\phi_I\,p_e d\Omega \quad (32)$$

In which u_{sf} is the structural displacement component perpendicular to the fluid boundary. Now, the whole assembled system of equations using the displacement potentials and displacements as the field variables in the fluid and solid domains leads to

$$\begin{bmatrix}\mathbf{M}_s & \mathbf{M}_c\\ 0 & \mathbf{M}_f\end{bmatrix}\begin{Bmatrix}\ddot{\mathbf{U}}_s\\ \ddot{\mathbf{\Psi}}\end{Bmatrix}+\begin{bmatrix}\mathbf{K}_s & 0\\ -\mathbf{K}_c & \mathbf{K}_f\end{bmatrix}\begin{Bmatrix}\mathbf{U}_s\\ \mathbf{\Psi}\end{Bmatrix}=\begin{Bmatrix}\mathbf{L}_s\\ -\mathbf{L}_e\end{Bmatrix} \quad (33)$$

Numerical results

5.1 Frequency analysis of a dam-reservoir system

In the first example, free vibration of the Pine Flat dam is considered (Calayir and Dumanoglu 1992). This example has been previously studied by many researchers (Greeves and Dumanoglu 1989, Chakrabarti and Chopra 1973). The dimensions of the problem are shown in Fig 2. The slop of the reservoir bed is assumed to be 0.05 in 1.0. The upstream face of the dam is assumed to be vertical. H=116.12 m is the reservoir height. The dam-reservoir system is considered over a rigid and horizontal foundation.. The displacements of the interface of dam-reservoir system are assumed to be equal in normal direction for the solid and fluid domains. Three different reservoir length L, are considered for the problem (L=H, L=2H and L=3H). We assume the boundary condition on the truncated boundary as the rigid stationary boundary.

The mass density, the elasticity modulus and poisson's ratio of the dam are taken as 2500 kg/m^3, 355×10^8 N/m^2 and 0.2, respectively. The water is taken as compressible and inviscid fluid with the bulk modulus, mass density and speed of sound are taken as 207×10^7 N/m^2, 1000 kg/m^3 and 1430 m/s, respectively.

The first mode shapes of the solid and fluid part of the problem are shown in Fig. 3, 4. The problem is solved for three different cases. As the first case, the natural frequencies of the solid domain (dam) without fluid are calculated. In the second case, the frequencies of the fluid domain without any interaction with the solid are investigated. Finally, as the third case, the elastic solid (dam) with water is investigated that means the fluid-structure interaction is considered. The computed frequencies for dam, reservoir and dam-reservoir system are shown in Tab. 1 (for reservoir length L=H). It should be noted that the finite element results given in this table are obtained using 8-node solid elements.

It should also be noted that the first frequency obtained from the present study for L=3H is 2.97 Hz which is close to the value 2.90 Hz obtained by Chakrabarti and Chopra (1973) and is also close to value 3.24 Hz obtained by Greeves and Dumanoglu (1989). The comparison between the results of the present study and those obtained by Chakrabarti and Chopra for various reservoir lengths are also shown in Tab. 2. The first and second frequencies of the coupled system with various reservoir lengths are also given in Tab. 3.

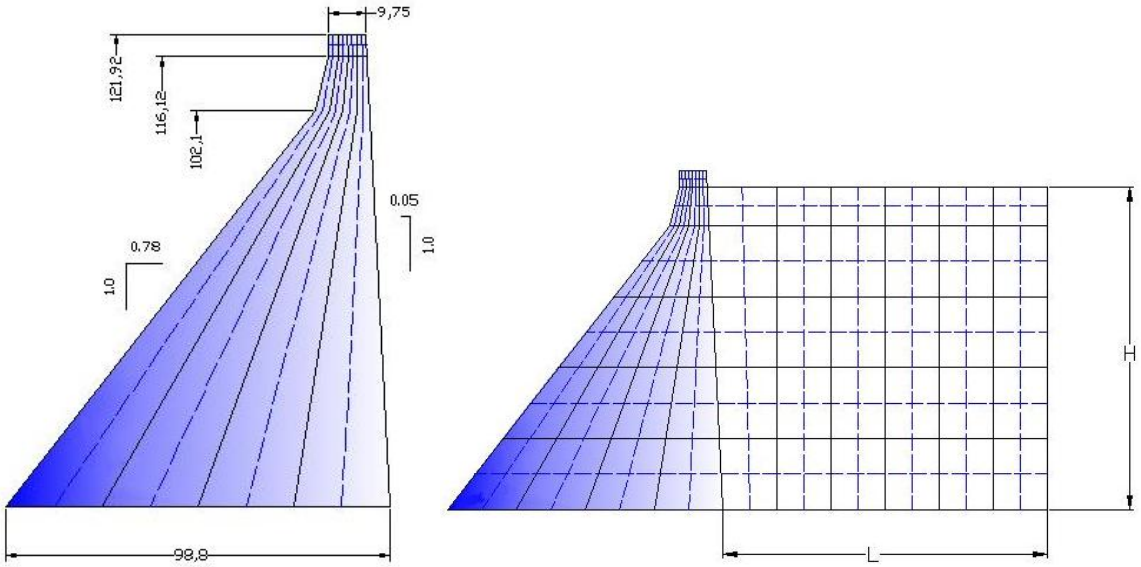

Figure 2. Dimensions and Model of Pine Flat Dam

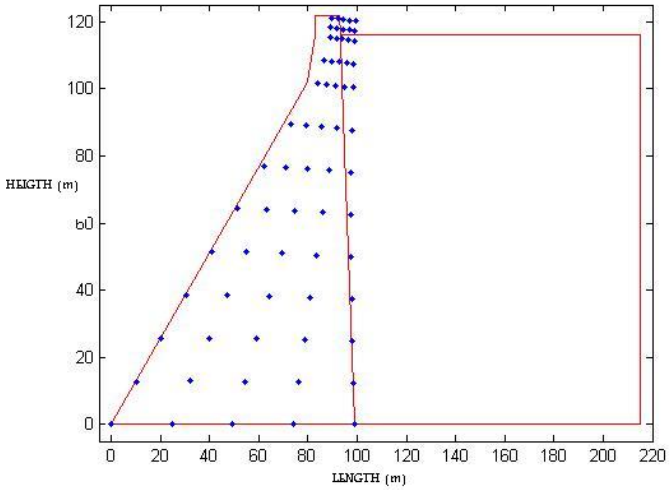

Figure 3. 1st mode shape of Model of Pine Flat Dam

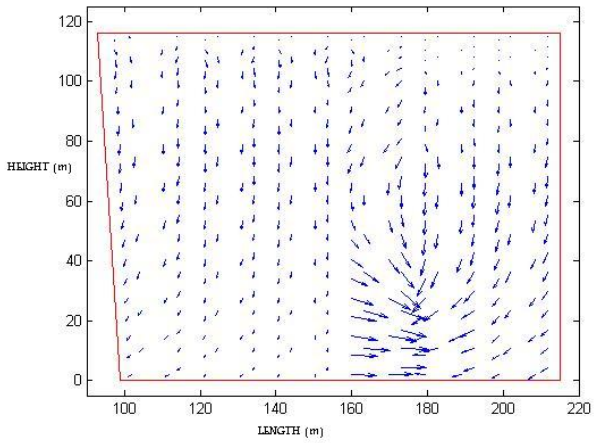

Figure 4. 1st mode shape of fluid in Pine Flat Dam

5. 2 Free vibration analysis of rectangular liquid storage structures

Free vibration analysis of two different types of rectangular liquid storage structures are considered as the second example. The first structure is a tall tank 10m wide and 15m tall, and the second one is a broad tank 30m wide with the same height. The wall thickness is taken to be 1.2m for both structures. The storage structures are assumed to be filled with water up to 13m (height) above the base. The actual dimensions of tanks are given in Fig. 5. The interaction surface is assumed to be vertical. The relative motion of the fluid along the wall is allowed only in the tangential

direction to the wall. The system is considered over a rigid and horizontal foundation. The natural element model consists 502 nodes including 96 and 434 solid and fluid nodes, respectively and 28 common nodes on the interaction surface. The solid is assumed to be homogeneous and isotropic. The material properties of the reinforced concrete storage structures are $E=1.962\times10^{10}$ N/m^2 , $\rho=2400$ kg/m^3 and $\nu=0.18$. The water is taken as compressible and inviscid fluid with the bulk modulus, mass density and speed of sound as 207×10^{7} N/m^2 , 1000 kg/m^3 and 1430 m/s, respectively.

The first mode shapes for two tanks are shown in Fig. 6 to 9. These example has been previously studied by Kim and Yun (1997). The comparison between their results and the present results are shown in Tab. 4. Good agreements can be observed between the results calculated by two different approaches. It can be seen from Table 4 that the natural element method predicts the first frequency of the broad tank as 2.04 Hz which is in good agreement with the value 2.12 Hz (Kim and Yun 1997). The same statement is true for the first frequency of the tall tank obtained by the natural element method and previous work (Kim and Yun 1997).

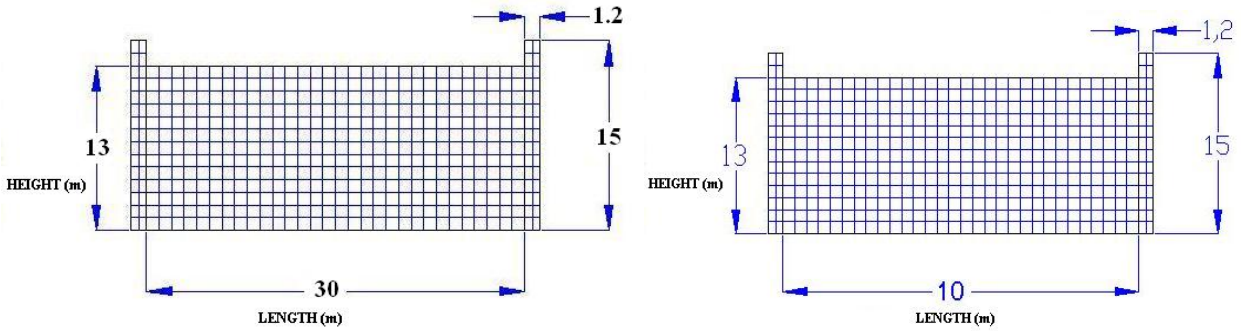

Figure 5. Dimensions of Tanks

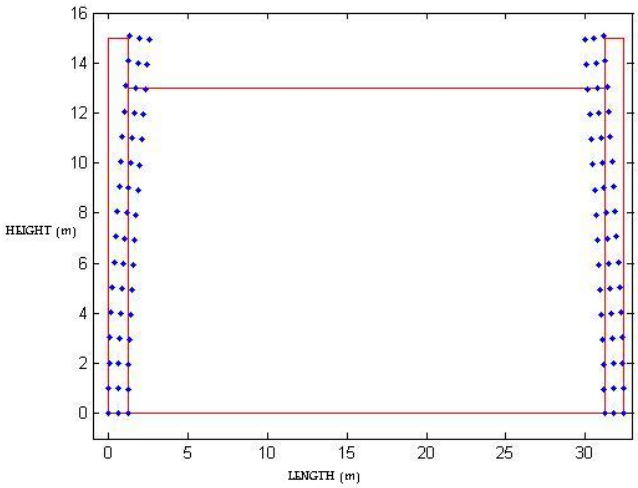

Figure 6. . 1st mode shape of Broad Tank

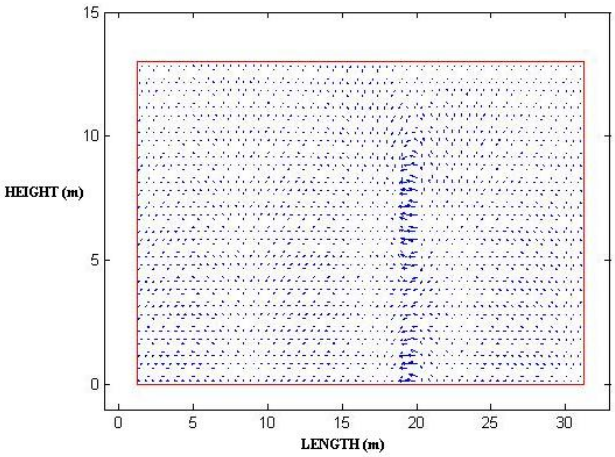

Figure 7. 1st mode shape of fluid in Broad Tank

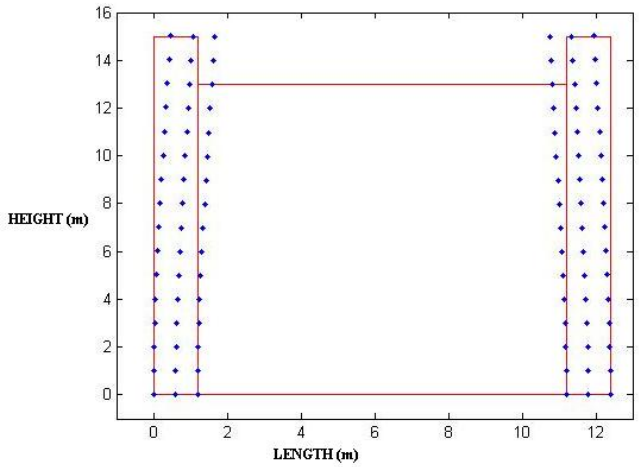

Figure 8. 1st mode shape of Tall Tank

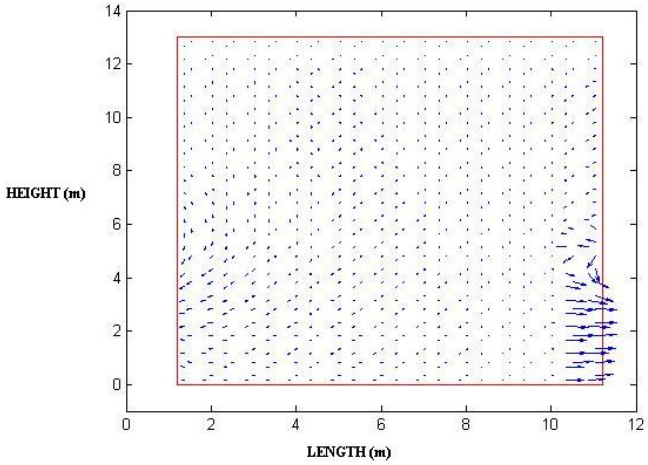

Figure 9. 1st mode shape of fluid in Tall Tank

Conclusion

Meshless methods have constituted an active field of research during the past decade, and have lead to many new and novel developments within computational mechanics. One of these methods, coined as the natural element method (NEM) or in its generality referred to as natural neighbour Galerkin methods, presents a few distinct and attractive features among meshless methods. The review of the NEM and its applications in free vibration analysis of fluid structure interaction problems has been the subject of this paper. In spite of previous efforts, the use of natural element method in solving such problems is a new idea and has not been considered so far. A comprehensive review of the method is conducted, including a description of the Sibson and the Laplace interpolants in two- and three-dimensions. Natural neighbour Galerkin methods use natural neighbour interpolation (either Sibson or Laplace interpolation) to construct the Galerkin discrete system of equations. These interpolate nodal data and are precisely linear on the boundary, and hence the imposition of essential boundary conditions can be carried out as is done in finite element method. This is in contrast to many meshless methods (such as element-free Galerkin method or those based on radial basis functions), in which the interpolating character is absent.

In conclusion, it is the authors' belief that natural neighbour-based techniques provide an appealing choice for many engineering problems and are a potential alternative to finite element method as well as some of the other meshless methods in computer modeling and simulation of complex phenomena in fluid structure interaction problems.

References

1. Alfaro, I., Bel, D., Cueto, E., Doblare, M., Chinesta, F. (2005) "Three-dimensional simulation of aluminium extrusion by the alpha-shape based natural element method", Computer Methods in Applied Mechanics and Engineering (accepted for publication).

2. Aliabadi, S., Johnson, A., and Abedi, J. (2003a) "Comparison of finite element and pendulum models for simulation of sloshing", Computers in Fluids, Vol. 32, p.p. 535–545

3. Aliabadi, S., Abedi, J., Zellars, B., Bota, K., and Johnson, A. (2003b) "Simulation technique for wave generation." Communications for Numerical Methods in Engineering, Vol. 19, p.p. 349–359

4. Aliabadi, S., Abedi, J., and Zellars, B. (2003c) "Parallel finite element simulation of mooring forces on floating objects", International Journal for Numerical Methods in Fluids, Vol. 41, p.p. 809–822

5. Aluru, N. R. (2000) "A point collocation method based on reproducing kernel approximations", International Journal for Numerical Methods in Engineering, Vol. 47, p.p. 1083-1121

6. De, S., Bathe, K. J. (2000) "The method of finite spheres", Computational Mechanic, Vol. 25, p.p. 329-345

7. Aluru, N. R., Li, G. (2001) "Finite cloud method: A true meshless technique based on a fixed reproducing kernel approximation", International Journal for Numerical Methods in Engineering, Vol. 50(10), p.p. 2373-2410

8. Atluri, S. N., Zhu, T. L. (2000) "New Concepts in Meshless Methods" International Journal for Numerical Methodsin Engineering, Vol. 47(1-3), p.p. 537-556

9. Babuska, I., Melenk, J. M. (1995) "The partition of unity finite element method" Technical Note EN-1185 Institute for Physical Science and Technology, University of Maryland

10. Belikov, V. V., Semenov, A. (2000) "Non-Sibsonian interpolation on arbitrary system of points in Euclidean space and adaptive isolines generation", Applied Numerical Mathematics, Vol. 32(4), p.p. 371–387

11. Belytschko, T., Lu, Y.Y., Gu, L. (1994a) "Element-free Galerkin methods", International Journal for Numerical Methods in Engineering, Vol. 37, p.p. 229-256

12. Bermudez, A., Rodriguez, R. (1994) "Finite element computation of the vibration modes of a fluid-solid system", Computer Methods in Applied Mechanics and Engineering, Vol. 119, p.p. 355-370

13. Bermudez, A., Duran, R., Rodriguez, R (1997) "Finite element solution of incompressible fluid-structure vibration problems", International Journal for Numerical Methods in Engineering, Vol. 40, p.p. 1435-1448

14. Calayir Y., Dumanoglu A. A. (1992) "Static and dynamic analysis of fluid and fluid-structure systems by the lagrangian method", International Journal for Computers & Structures, Vol. 49, No. 4, p.p. 625-632.

15. Chakrabarti P., Chopra A. K. (1973) "Earthquake analysis of gravity dams including hydrodynamic interaction", Earthquake Engineering Structures, Dyn. 2, 143-160.

16. Cueto, E., Sukumar, N., Calvo, B., Martinez, M.A., Cegonino, J., Doblare, M. (2003) "Overview and recent advances in natural neighbour Galerkin methods", Archives of Computational Methods in Engineering, Vol. 10 No.4, p.p. 307-384

17. Daneshmand, F., Sharan, S.K., Kadivar, M.H. (2004) "Dynamic analysis of a gate-fluid system", ASCE Journal of Engineering Mechanics, Vol. 130, p.p. 1458-1466

18. Daneshmand, F., Niroomandi, S. (2007) "Natural neighbour Galerkin computation of the vibration modes of fluid-structure systems", Engineering Computations, Accepted.

19. Farin, G. (1990) "Surfaces over Dirichlet tessellations", Computer Aided Geometric Design, Vol. 7(1-4), p.p. 281–292

20. Greeves E. J., Dumanoglu A. A. (1989) "The implementation of an efficient computer analysis for fluid-structure interaction using the Eulerian approach within SAP-IV", Department of Civil Engineering, University of Bristol, Bristol.

21. Hiyoshi, H., Sugihara, K., (2002) "Improving continuity of Voronoi-based interpolation over Delaunay spheres", Computational Geometry, Vol. 22, p.p. 167–183

22. Kim Y. S., Yun C. B. (1997) "A spurious free four-node displacement-based fluid element for fluid-structure interaction analysis", International Journal for Engineering Structures, Vol. 19, No. 8, p.p. 665-678.

23. Liu, W. K., Chen, Y. (1995b), "Wavelet and multiple scale reproducing Kernel methods", International Journal for Numerical Methods in Fluids, Vol. 21, p.p. 901– 933

24. Liu, W. K., Jun S. and Zhang, Y. F. (1995) "Reproducing Kernel particle methods", International Journal of Numerical Methods in Fluids, Vol. 20, p.p.1081–1106

25. Liu, W. K., Jun, S., Li, S., Adee, J. and Belytschko, T. (1995a) "Reproducing Kernel particle methods for structural dynamics", International Journal for Numerical Methods in Engineering, Vol. 38, p.p. 1655–1679

26. Lu, Y., Belytschko, T., Gu, L. (1994b), "A new implementation of the element free Galerkin method", Computational Methods in Applied Mechanics and Engineering, Vol. 113, p.p. 397– 414

27. Monaghan, J. J.(1988) "An introduction to SPH", Computational Physics Communications, Vol. 48, p.p. 89-96

28. Nayroles, B., Touzot, G., Villon P. (1992) "Generalizing the FEM: Diffuse approximation and diffuse elements", Computational Mechanics, Vol. 10, p.p. 307-18

29. Onate, E., Idelsohn, S. R. and Zienkiewicz O. C. (1996a) "A finite point method in computational mechanics: Applications to convective transport and fluid flow", International Journal for Numerical Methods in Engineering, Vol. 39, p.p. 3839-3866.

30. Onate, E., Idelsohn, S., Zienkiewicz, O.C., Taylor, R.L., Sacco, C. (1996b) "A stabilized finite point method for analysis of fluid mechanics problems", Computer Methods in Applied Mechanics and Engineering, Vol. 139, p.p. 315-346

31. Piper, P. (1993) "Properties of local coordinates based on Dirichlet tessellations", In G. Farin, H. Hagen, and H. Noltemeier, editors, Geometric Modeling, Vol. 8, p.p. 227–239, Springer-Verlag.

32. Sibson, R. (1980) "A vector identity for the Dirichlet Tessellation", Mathematical Proceedings of the CambridgePhilosophical Society, Vol. 87(1), p.p. 151-155

33. Sukumar, N., Moran, B., Semenov, A., Belikov, V. V. (2001) "Natural neighbour Galerkin Methods", International Journal for Numerical Methods in Engineering, Vol. 50, p.p. 1-27.

34. Wang, X., Bathe, K.J. (1997) "Displacement/Pressure based mixed finite element formulations for acoustic fluid-structure interaction problems", International Journal for Numerical Methods in Engineering, Vol. 40, p.p. 2001-2017

TABLES:

Table 1. Frequencies (Hz) for Dam, Reservoir and Dam-Reservoir system (L=H)

Mode	Solid (Dam)		Fluid (Reservoir)		Dam-Reservoir	
	NEM	FEM	NEM	FEM	NEM	FEM
1	4.18	4.12	3.10	3.05	2.87	3.03
2	9.19	8.76	6.89	6.75	3.92	3.90
3	11.11	11.06	9.24	9.16	6.76	6.77
4	15.94	15.00	11.10	10.85	8.92	8.54
5	23.50	22.63	13.09	12.80	9.41	9.26

Table 2. Fundamental Frequency (Hz) for Dam-Reservoir system

Mode	Dam-Reservoir system	
	Present Study	Chakrabarti and Chopra (REF)
L=H	2.87	2.78
L=2H	2.94	2.87
L=3H	2.97	2.89

Table 3. Frequencies (Hz) for Dam-Reservoir system

Mode	L=H	L=2H	L=3H
1	2.87	2.94	2.97
2	3.92	3.63	3.41

Table 4. Frequencies of the storage tanks (Hz)

Mode	Tall tank		Broad tank	
	Present	REF	Present	REF
1	2.12	2.05	2.04	1.98
2	10.35	11.41	10.57	10.50
3	31.81	31.76	28.80	30.97